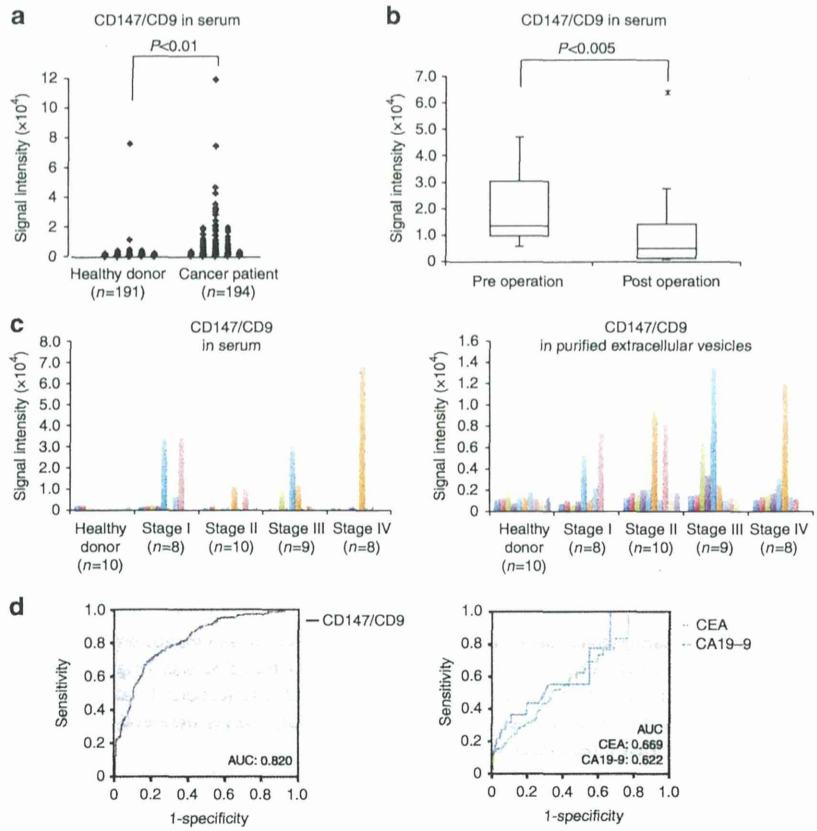

Figure 6 | Analysis of circulating CD147 and CD9 double-positive EVs in healthy donors or colorectal cancer patient sera. (**a**) Serum levels of CD147/CD9 double-positive EVs in colorectal cancer patients without any purification. The panel shows a scatter plot for healthy donors ($n=191$) and colorectal cancer patients ($n=194$). The *P*-value was calculated by using Wilcoxon rank-sum test. (**b**) Changes in serum levels of CD147/CD9 double-positive EVs in colorectal cancer patients (stage I or II: $n=15$) before (preoperation) and after (postoperation after 7–34 days) surgical removal of the tumor. Box lengths represent the interquartile range (first to third quartiles). The line in the center of the boxes represents the median value. Data represented by the asterisks are extreme values (greater than three times the interquartile range over the third quartile). The *P*-value was calculated by using Wilcoxon signed-rank test. (**c**) The results of ExoScreen detection of circulating EVs (left panel) and purified circulating EVs (right panel) in sera from healthy donors ($n=10$) and colorectal cancer patients ($n=35$) using CD147 and CD9 antibodies. The panels show the signal intensities from each samples measured for CD147/CD9 double-positive EVs using ExoScreen. (**d**) Receiver operating characteristic curves between healthy donors and colorectal cancer patients assesing by CD147/CD9 double-positive EVs (left panel), CEA and CA19-9 (right panel). left panel, CD147/CD9 double-positive EVs (healthy donors versus colorectal cancer patients; AUC: 0.820); right panel, CEA (AUC: 0.669); CA19-9 (AUC: 0.622) Data are representative of at least three independent experiments each. AUC, area under the curve.

Notably, CD147 is plasma membrane protein and this is suitable for applying to the ExoScreen. We observed that CD147 is expressed on all of the colorectal cancer cell lines, but their expression levels are not uniform (Fig. 5a,b and Supplementary Figs 7 and 8). In addition, CD147 in EVs from CCD-18Co cells was hardly detectable. Several reports have shown that CD147 is expressed in the majority of human tumour types including colorectal cancer[17,18], although CD147 is expressed in a variety of embryonic and adult tissues, such as spermatocytes, neuronal cells, erythrocyte and so on[19]. In addition, CD147 functions in lactate transporter, which is an important feature of cancer cell, because of the excessive anaerobic glycolysis phenomenon in cancer cells referred to as the Warburg effect[20]. Indeed, associations between high expression of CD147 and poor prognosis have previously been shown in colorectal cancer[21], thus representing a potential marker for *ex vivo* analysis of tumour-derived EVs.

CD147 and CD9 double-positive EVs in clinical samples. Next, we used ExoScreen to detect cancer-derived EVs in human clinical samples (Fig. 6a). As shown in Fig. 6a, we found that CD147 and CD9 double-positive EVs were significantly higher in serum from cancer patients ($n=194$) than in serum from healthy donors ($n=191$). Most importantly, most of CD147 in cancer patient sera reduced after surgery (Fig. 6b), suggesting that the reduced signal of CD147 obtained from ExoScreen is originated from cancer-derived EVs, even the variety of cells expressed CD147. To confirm whether by ExoScreen really reflects the protein profile of EVs in circulation, EVs were purified from the sera of tumour patients ($n=35$) and healthy donors ($n=10$) and analysed for expression of CD147 via immunoblotting (Supplementary Fig. 9). We also performed ExoScreen against the same serum samples obtained by ultracentrifugation (Fig. 6c, right panel). As depicted in Supplementary Fig. 9, the expression of CD147 in EVs isolated from the sera of cancer patients correlated clearly with the results obtained from the ExoScreen assay (Fig. 6c), indicating that the accuracy of ExoScreen was confirmed and that it can be used to monitor EVs in circulation without any purification. Taken together, these results demonstrate that ExoScreen can be a tool for detection of EVs from as little as 5 µl of cancer patients' serum to detect circulating cancer-derived EVs.

Discussion

In summary, we propose a rapid, highly sensitive and widely usable detection method based on the amplified luminescent proximity homogeneous assay using photosensitizer-beads for cancer cell-derived EVs. Notably, different antibodies can be conjugated to capture different analytes, such as CD147, thus various types of cancer can be targetd. There are various colorectal cancer screening tests. For example, the fecal occult blood test has been recommended widely as a screening test for colorectal cancer; however, the fecal occult blood displays low sensitivity and specificity for detecting colorectal cancer[22]. Moreover, carcinoembrionic antigen (CEA) and carbohydrate antigen 19-9 (CA19-9) are the most commonly used tumour-associated antigens in the management of patients with colorectal cancer, although those biomarkers are not sensitive enough for early colorectal cancer[23,24]. In fact, the high levels of CD147 detected in patient sera showed the normal value range of CEA and CA19-9 in stage I patients (Supplementary Tables 2 and 3). In addition, the receiver operating characteristic curve indicates a diagnostic advantage of CD147/CD9 double-positive EVs in comparison with CEA and CA19-9 (Fig. 6d). From these aspects and the result shown in Fig. 6b, ExoScreen detecting CD147/CD9 double-positive EVs might be used for monitoring the status of cancer after the surgery and during chemotherapy, resulting in increase in QOL of the patients and providing doctor for the proper assessment of patient status. Further studies are needed to know whether our ExoScreen reduces colorectal cancer mortality as a screening test. It should be noted that CD147/CD9 double-positive EVs were also detected in samples with early stage colorectal cancer that invade into submucosal layer (T1 stage according to UICC classification) (Supplementary Table 2) by the ExoScreen assay. These results also indicate that ExoScreen can be used to detect biomarkers for diseases that are currently difficult to diagnose and monitor not only cancer, but autoimmune disease and degenerative disease of the brain. Thus, our data suggest that ExoScreen, in addition to being a novel liquid biopsy platform for the detection of circulating EVs, may aid variety of disease diagnosis and help to identify companion biomarkers that are important for new drug development.

Methods

Cell cultures. Human colorectal cancer cell lines (HCT116 cells, HCT15 cells, HT29 cells, COLO201 cells, COLO205 cells, WiDr cells and SW1116 cells) and normal colon fibroblast cell line CCD-18Co cells were purchased from American Type Culture Collection. HCT116 and HT29 cells were cultured in McCoy's 5A medium supplemented with 10% heat-inactivated fetal bovine serum (FBS) and an antibiotic–antimycotic solution (Invitrogen) at 37 °C in 5% CO_2. WiDr cells CCD-18Co cells were cultured in minimal essential medium (MEM) containing 2 mM L-gulutamine, an antibiotic–antimycotic solution, nonessential amino acids and 10% FBS at 37 °C in 5% CO_2. HCT15 cells, COLO201 cells and COLO205 cells were cultured in RPMI 1640 medium supplemented with 10% heat-inactivated FBS and an antibiotic–antimycotic solution at 37 °C in 5% CO_2. SW1116 cells were cultured in Leibovitz' L15 medium supplemented with 10% heat-inactivated FBS and an antibiotic–antimycotic solution at 37 °C in without CO_2. The following additional cell lines were used: PNT2 cells, an immortalized normal adult prostatic epithelial cell line (DS Pharma Biomedical Co., Ltd. Osaka, Japan); PC3 cells, a human prostate cancer cell line initiated from a bone metastasis of a grade IV prostatic adenocarcinoma (American Type Culture Collection); MDA-MB-231-luc-D3H2LN cells (MDA-MB-231LN), a highly metastatic human breast cancer cell line (Xenogen); and MCF7 cells, a human breast cancer cell line which expresses oestrogen receptor (American Type Culture Collection). The above cells were cultured in RPMI 1640 medium supplemented with 10% FBS and an antibiotic–antimycotic solution at 37 °C in 5% CO_2.

Patient serum samples. Collection and usage of human serum from corolectal cancer patients ($n = 194$) and healthy donor ($n = 94$) were approved by Osaka university Institutional Review Board (No.11343). Serum was aliquoted and kept at − 80 °C until used, and freeze-thawing was avoided as much as possible after that. Some part of the serum samples ($n = 97$) from healthy donor shown in Fig. 6a were purchased from BizCom Japan (Tokyo, Japan). Serum samples containing red blood cells were excluded from the analysis. Informed consent was obtained from all patients.

Preparation of conditioned media and EVs. The cells were washed with phosphate-buffered saline (PBS), and the culture medium was replaced with advanced Dulbecco's Modified Eagle Medium for HCT116 cells, WiDr cells, SW1116 cells, HT29 cells and CCD-18Co cells, or advanced RPMI medium for the other cell lines, containing an antibiotic–antimycotic and 2 mM L-glutamine (but not containing FBS). After incubation for 48 h, the CM was collected and centrifuged at 2,000 *g* for 10 min at 4 °C. To thoroughly remove cellular debris, the supernatant was filtered through a 0.22 μm filter (Millipore). The CM was then used for EV isolation. To prepare EVs, CM or the sera from colorectal patients and healthy donors were ultracentrifuged at 110,000 *g* for 70 min at 4 °C. The pellets were washed with 11 ml of PBS, ultracentrifuged at 110,000 *g* for 70 min at 4 °C and resuspended in PBS. The putative EVs fraction was measured for its protein content using a Quant-iT Protein Assay with Qubit2.0 Fluorometer (Invitrogen).

Reagents. The following antibodies were used for immunoblotting: mouse monoclonal anti-human CD63 antibody (clone H5C6, dilution 1:200) from BD Biosciences, mouse monoclonal anti-human CD9 antibody (clone ALB 6, dilution 1:200) from SantaCruz Biotechnology, mouse monoclonal anti-human CD147 antibody (clone MEM-M6/1, dilution 1:1,000) from Novus Biologicals and mouse monoclonal anti-Actin (clone C4, dilution 1:1,000) from Millipore. The secondary antibody (horseradish peroxidase-labeled sheep anti-mouse) were purchased from GE HealthCare.

The following antibodies used for ExoScreen and ELISA were developed in Shionogi & Co., LTD.: mouse monoclonal anti-human CD63 antibody (clone 8A12) and mouse monoclonal anti-human CD9 antibody (clone 12A12). Mouse monoclonal anti-human CD147 antibody (clone MEM-M6/1) was purchased from Novus Biologicals. Antibodies were used to modify either acceptor bead or biotin following the manufacturer's protocol.

AlphaLISA reagents (Perkin Elmer, Inc., Waltham, MA 02451, USA) consisted of AlphaScreen Streptavidin-coated donor beads (6760002), AlphaLISA Unconjugated-acceptor beads (6062011) and AlphaLISA Universal buffer (AL001F). AlphaLISA assays were performed in 96-well half-area white plates (6005560) and read in an EnSpire Alpha 2300 Multilabel Plate reader (Perkin Elmer, Inc.).

ExoScreen assay. A 96-well half-area white plate was filled with 5 μl of sample, 5 nM biotinylated antibodies and 50 μg ml^{-1} AlphaLISA acceptor beads conjugated antibodies in the universal buffer. The volume of each reagent was 10 μl. The plate was then incubated for 1–3 h at room temperature. Without a washing step, 25 μl of 80 μg ml^{-1} AlphaScreen streptavidin-coated donor beads were added. The reaction mixture was incubated in the dark for another 30 min at room temperature and the plate was then read on the EnSpire Alpha 2300 Multilabel Plate reader using an excitation wavelength of 680 nm and emission detection set at 615 nm. Background signals obtained from PBS were subtracted from the measured signals.

ELISA. Ninety-six well-plates (Nunc) were coated with 2.5 μg ml^{-1} anti-human CD9 or -CD63 antibodies in a volume of 50 μl per well of carbonate buffer (pH 9.6) and incubated for 4 h at room temperature. After 2 washes with 0.01% Tween-20 in PBS, 100 μl per well of Blocking One solution (Nacalai Tesque) was added at room temperature for 1 h. Following 3 washes in PBS, EVs purified from cell culture supernatants were added in a final volume of 50 μl and incubated for 1 h at room temperature. After 3 washes with PBS, 50 μl of biotinylated anti-human CD9 or -CD63 antibodies diluted to 1 μg ml^{-1} were added and incubated for 1 h at room temperature. After 3 washes with PBS, the plate was incubated with 100 μl of HRP-conjugated streptavidin (Cell Signalling Technology) diluted 1:2,000 in Blocking One solution for 1 h at room temperature. After the final 3 washes with PBS, the reaction was developed with Peroxidase (TMB One Component HRP Microwell Substrate, SurModics). The reaction was arrested with 450 nm Stop Reagent for TMB Microwell Substrates (SurModics) and optical densities were recorded at 450 nm.

Immunoblotting. Equal amounts of EVs or whole-cell lysates were loaded onto 4–15% Mini-PROTEAN TGX gels (Bio-Rad, Munich, Germany). Following electrophoresis (100 V, 30 mA), the proteins were transferred to a polyvinylidene difluoride membrane. The membranes were blocked with Blocking One solution and then incubated with primary antibodies. After washing, the membranes were incubated with horseradish peroxidase-conjugated sheep anti-mouse IgG and then subjected to enhanced chemiluminescence using ImmunoStar LD (Wako). CD63, CD9 and CD147 were detected under non-reducing conditions. Original scans of the cropped images in the main figures (Figs 3a and 5a) are presented in Supplementary Fig. 10.

Measurement of size distribution by NTA. Nanoparticle tracking analysis (NTA) was carried out using the Nanosight system (NanoSight) on sera diluted 1000-fold with PBS for analysis. The system focuses a laser beam through a suspension of the particles of interest. These are visualized by light scattering using a conventional optical microscope aligned perpendicularly to the beam axis, which collects light scattered from every particle in the field of view. A 60 s video recorded all events for further analysis by NTA software. The Brownian motion of each particle was tracked between frames to calculate its size using the Stokes–Einstein equation.

References

1. Iero, M. *et al.* Tumour-released exosomes and their implications in cancer immunity. *Cell Death Differ.* **15,** 80–88 (2008).
2. Webber, J., Steadman, R., Mason, M. D., Tabi, Z. & Clayton, A. Cancer exosomes trigger fibroblast to myofibroblast differentiation. *Cancer Res.* **70,** 9621–9630 (2010).
3. Al-Nedawi, K. *et al.* Intercellular transfer of the oncogenic receptor EGFRvIII by microvesicles derived from tumour cells. *Nat. Cell Biol.* **10,** 619–624 (2008).
4. Skog, J. *et al.* Glioblastoma microvesicles transport RNA and proteins that promote tumour growth and provide diagnostic biomarkers. *Nat. Cell Biol.* **10,** 1470–1476 (2008).
5. Taylor, D. D. & Gercel-Taylor, C. MicroRNA signatures of tumor-derived exosomes as diagnostic biomarkers of ovarian cancer. *Gynecol. Oncol.* **110,** 13–21 (2008).
6. Peinado, H. *et al.* Melanoma exosomes educate bone marrow progenitor cells toward a pro-metastatic phenotype through MET. *Nat. Med.* **18,** 883–891 (2012).
7. Kosaka, N., Iguchi, H. & Ochiya, T. Circulating microRNA in body fluid: a new potential biomarker for cancer diagnosis and prognosis. *Cancer. Sci.* **101,** 2087–2092 (2010).
8. Raposo, G. & Stoorvogel, W. Extracellular vesicles: exosomes, microvesicles, and friends. *J. Cell Biol.* **200,** 373–383 (2013).
9. Mathivanan, S. & Simpson, R. J. ExoCarta: a compendium of exosomal proteins and RNA. *Proteomics* **9,** 4997–5000 (2009).
10. Bobrie, A. *et al.* Rab27a supports exosome-dependent and -independent mechanisms that modify the tumor microenvironment and can promote tumor progression. *Cancer Res.* **72,** 4920–4930 (2012).
11. Yoshioka, Y. *et al.* Comparative marker analysis of extracellular vesicles in different human cancer types. *J. Extracell. Vesicles* **2,** doi:10.3402/jev.v2i0.20424 (2013).
12. Valadi, H. *et al.* Exosome-mediated transfer of mRNAs and microRNAs is a novel mechanism of genetic exchange between cells. *Nat. Cell Biol.* **9,** 654–659 (2007).
13. Eglen, R. M. *et al.* The use of AlphaScreen technology in HTS: current status. *Curr. Chem. Genomics* **25,** 2–10 (2008).
14. Kosaka, N. *et al.* Neutral sphingomyelinase 2 (nSMase2)-dependent exosomal transfer of angiogenic microRNAs regulate cancer cell metastasis. *J. Biol. Chem.* **288,** 10849–10859 (2013).
15. Xiao, D. *et al.* Identifying mRNA, microRNA and protein profiles of melanoma exosomes. *PLoS One* **7,** e46874 (2012).
16. Choi, D. S. *et al.* Quantitative proteomics of extracellular vesicles derived from human primary and metastatic colorectal cancer cells. *J. Extracell. Vesicles* **1,** doi:10.3402/jev.v1i0.18704 (2012).
17. Riethdorf, S. *et al.* High incidence of EMMPRIN expression in human tumors. *Int. J. Cancer.* **119,** 1800–1810 (2006).
18. Li, Y. *et al.* HAb18G (CD147), a cancer-associated biomarker and its role in cancer detection. *Histopathology* **54,** 677–687 (2009).
19. Muramatsu, T. & Miyauchi, T. Basigin (CD147): a multifunctional transmembrane protein involved in reproduction, neural function, inflammation and tumor invasion. *Histol. Histopathol.* **18,** 981–987 (2003).
20. Weidle, U. H., Scheuer, W., Eggle, D., Klostermann, S. & Stockinger, H. Cancer-related issues of CD147. *Cancer. Genomics. Proteomics.* **7,** 157–169 (2010).
21. Boye, K. *et al.* EMMPRIN is associated with S100A4 and predicts patient outcome in colorectal cancer. *Br. J. Cancer.* **107,** 667–674 (2012).
22. Ahlquist, D. A. *et al.* Accuracy of fecal occult blood screening for colorectal neoplasia. A prospective study using Hemoccult and HemoQuant tests. *JAMA* **269,** 1262–1267 (1993).
23. Chapman, M. A., Buckley, D., Henson, D. B. & Armitage, N. C. Preoperative carcinoembryonic antigen is related to tumour stage and long-term survival in colorectal cancer. *Br. J. Cancer.* **78,** 1346–1349 (1998).
24. Kuusela, P. *et al.* Comparison of CA 19-9 and carcinoembryonic antigen (CEA) levels in the serum of patients with colorectal diseases. *Br. J. Cancer.* **49,** 135–139 (1984).

Acknowledgements

This work was supported in part by a Grant-in-Aid for the Third-Term Comprehensive 10-Year Strategy for Cancer Control, a Grant-in-Aid for Scientific Research on Priority Areas Cancer from the Ministry of Education, Culture, Sports, Science and Technology, and the Program for Promotion of Fundamental Studies in Health Sciences of the National Institute of Biomedical Innovation (NiBio), and the Japan Society for the Promotion of Science (JSPS) through the 'Funding Program for World-Leading Innovative R&D on Science and Technology (FIRST Program)' initiated by the Council for Science and Technology Policy (CSTP), and a Grant-in-aid for Project for Development of Innovative Research on Cancer Therapeutics (P-Direct), and Grant-in-Aid for Scientific Research on Innovative Areas ('functional machinery for non-coding RNAs') from the Japanese Ministry of Education, Culture, Sports, Science, and Technology, and Comprehensive Research and Development of a Surgical Instrument for Early Detection and Rapid Curing of Cancer Project (P10003) of the New Energy and IndustrialTechnology Development Organization (NEDO), a research program of the Project for Development of Innovative Research on Cancer Therapeutics (P-Direct), Ministry of Education, Culture, Sports, Science and Technology of Japan. We thank Ms. Ayako Irie at Quantum design Japan for supporting the Nanosight tracking analysis. We thank Ms. Ayako Inoue for excellent technical assistance. We thank Dr Roger Bosse and Dr Nami Kamura at Perkin Elmer for advising protocol for AlphaLisa system.

Author contributions

T.O. originated the concept. Y.Y., N.K. and T.O. carried out the project design. H.Oh., H.Ok. and H.S. developed the antibodies. R.N., H.Y., H.I., M.M., K.F. and T.N provided the serum samples. H.Ha., H.S., H.Hi., F.T. and T.K. assisted with data interpretation. Y.K. and Y.Y. performed the experiments and T.O. supervised the project; Y.Y., N.K. and T.O. contributed to the writing of the manuscript.

Additional information

Supplementary Information accompanies this paper at http://www.nature.com/naturecommunications

Competing financial interests: The authors declare no competing financial interests.

Reprints and permission information is available online at http://npg.nature.com/reprintsandpermissions/

How to cite this article: Yoshioka, Y. *et al.* Ultra-sensitive liquid biopsy of circulating extracellular vesicles using ExoScreen. *Nat. Commun.* 5:3591 doi: 10.1038/ncomms4591 (2014).

SUPPLEMENTARY INFORMATION

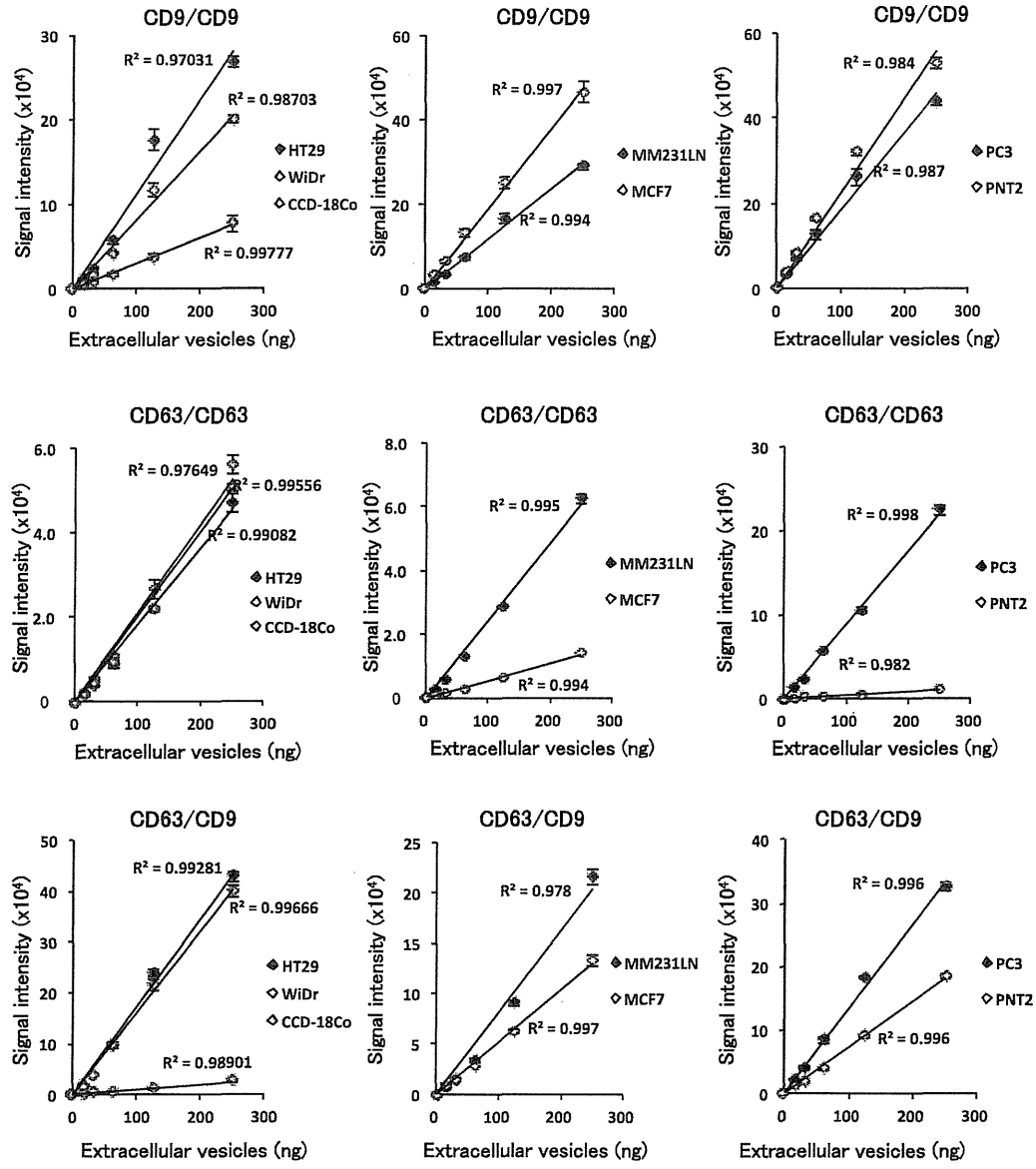

Supplementary Fig. 1. Correlation between ExoScreen measurements for CD9-positive, CD63-positive, or CD63/CD9 double-positive EVs and EV protein concentration in a dilution series. EV protein concentration was measured via the Qubit system, and EVs were purified from conditioned medium of the colorectal cancer cell lines HT29 and WiDr and normal colon fibroblast cell line CCD-18Co, PC3 prostate cancer cell line, PNT2 prostate epithelial cell line, and the breast cancer cell lines MDA-MB-231LN and MCF7. Error bars are s.e.m. (n=3 for each condition). Data are representative of at least three independent experiments each.

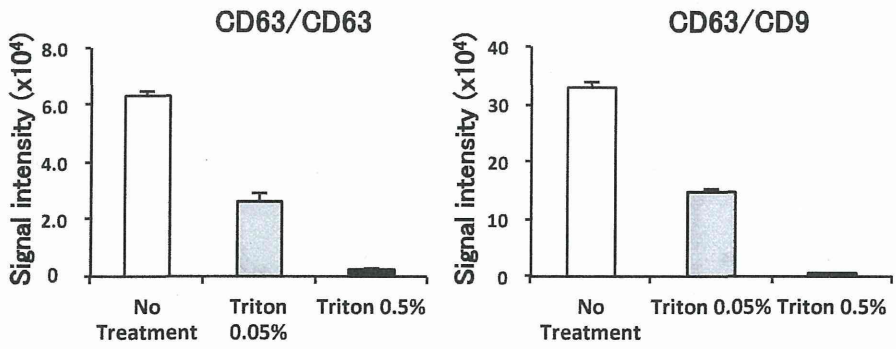

Supplementary Fig. 2. Evaluation of ExoScreen specificity against purified EVs from HCT116 cell treated with or without 0.05% and 0.5% Triton X-100. Two hundred fifty ng of EVs were detected by ExoScreen using CD63 antibodies (left panel) and, CD63 and CD9 antibodies (right panel). Error bars are s.e.m. (n=3 for each condition). Data are representative of at least three independent experiments each.

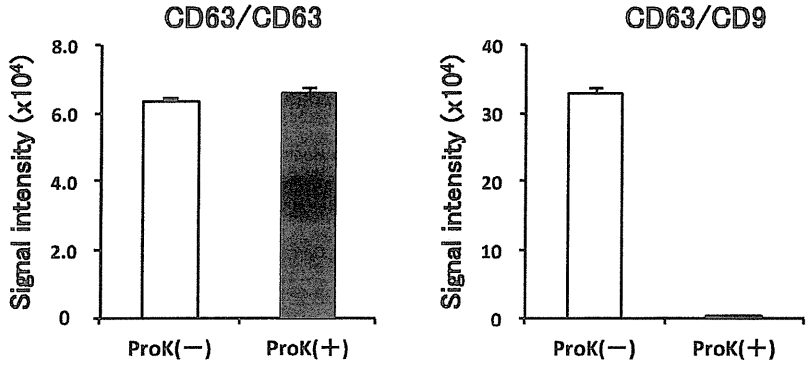

Supplementary Fig. 3. Evaluation of ExoScreen specificity against EVs from HCT116 cells treated with or without Proteinase K. Two hundred fifty ng of EVs were detected by ExoScreen using CD63 antibodies (left panel) and, CD63 and CD9 antibodies (right panel). Error bars are s.e.m. (n=3 for each condition). Data are representative of at least three independent experiments each.

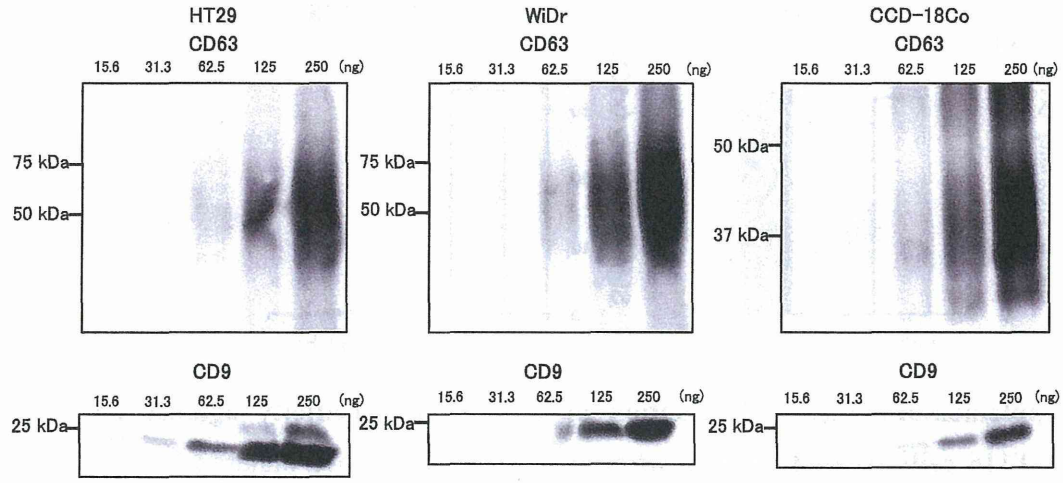

Supplementary Fig. 4. Immunoblotting analysis of CD63 (upper panels) or CD9 (lower panels) against the EVs isolated from HT29, WiDr and CCD-18Co cells. EV protein concentrations were measured via the Qubit system. EVs were purified from HT29, WiDr and CCD-18Co cell conditioned medium. Data are representative of at least three independent experiments each.

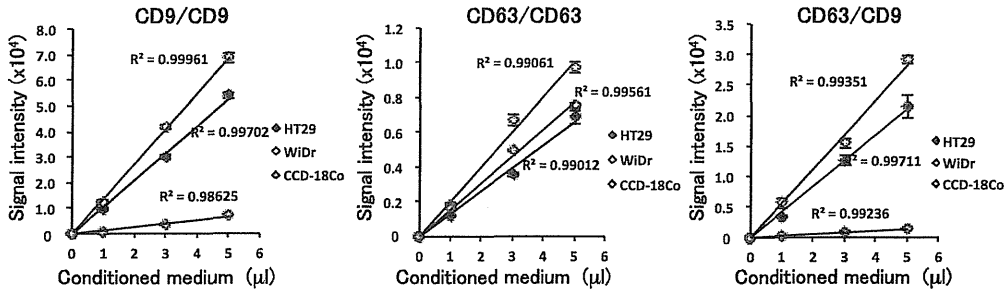

Supplementary Fig. 5. Correlation of ExoScreen measurements for CD9-positive, CD63-positive or CD63/CD9 double-positive EVs and HT29, WiDr and CCD-18Co conditioned medium in a dilution series. Conditioned medium was prepared in a 5 µl volume and diluted as indicated. EVs in conditioned medium were detected by ExoScreen using CD9 antibodies (left panel), CD63 antibodies (middle panel) and, CD63 and CD9 antibodies (right panel). Error bars are s.e.m. (n=3 for each condition). Data are representative of at least three independent experiments each.

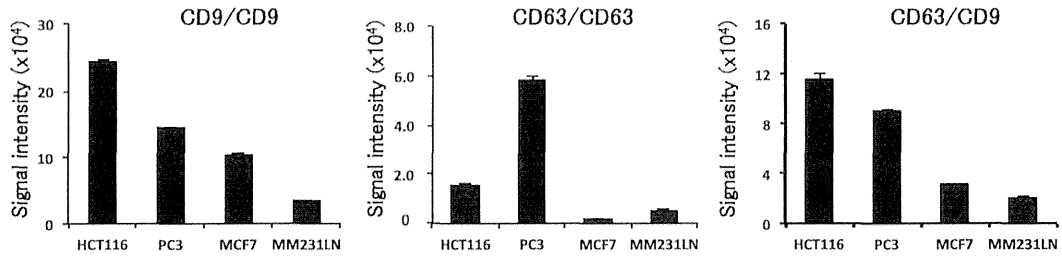

Supplementary Fig. 6. Detection of EVs in 5 μl of conditioned medium from indicated cancer cell lines without purification of EVs. EVs in conditioned medium were detected by ExoScreen using CD9 antibodies (left panel), CD63 antibodies (middle panel) and, CD63 and CD9 antibodies (right panel). Error bars are s.e.m. (n=3 for each condition). Data are representative of at least three independent experiments each.

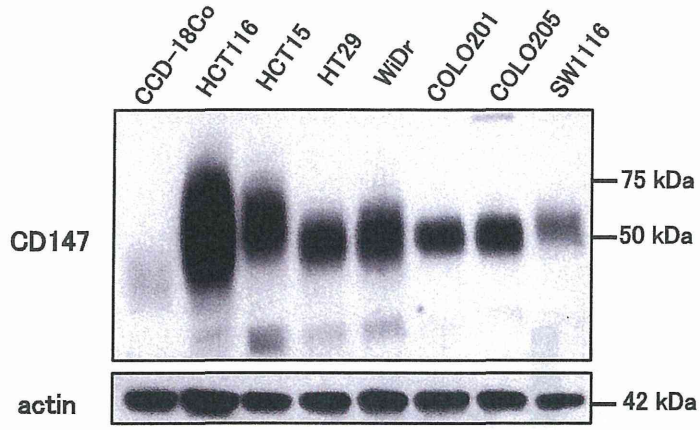

Supplementary Fig. 7. Immunoblotting analysis of CD147 or actin against cell lysates from CCD-18Co cells, HCT116 cells, HCT15 cells, HT29 cells, WiDr cells, COLO201 cells, COLO205 cells and SW1116 cells. Cell lysate (1 μg per lane) was used for the detection of actin. CD147 was detected using 5 μg of whole cell lysates. Data are representative of at least three independent experiments each.

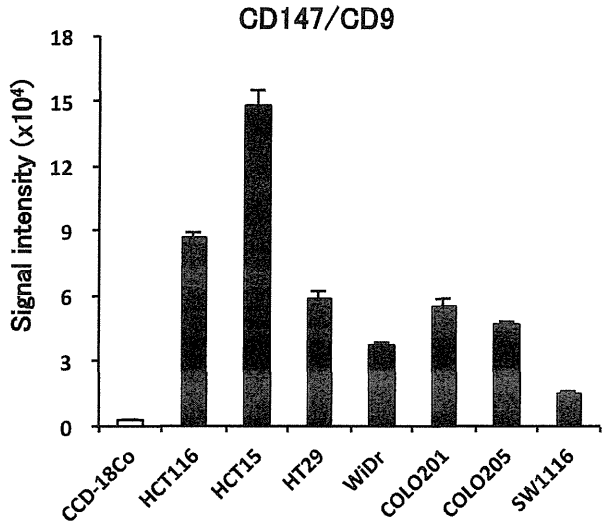

Supplementary Fig. 8. Purified EVs from indicated cell lines was used for the detection of CD147/CD9 double-positive EVs. EVs (62.5 ng) were detected by ExoScreen using CD147 and CD9 antibodies. Error bars are s.e.m. (n=3 for each condition). Data are representative of at least three independent experiments each.

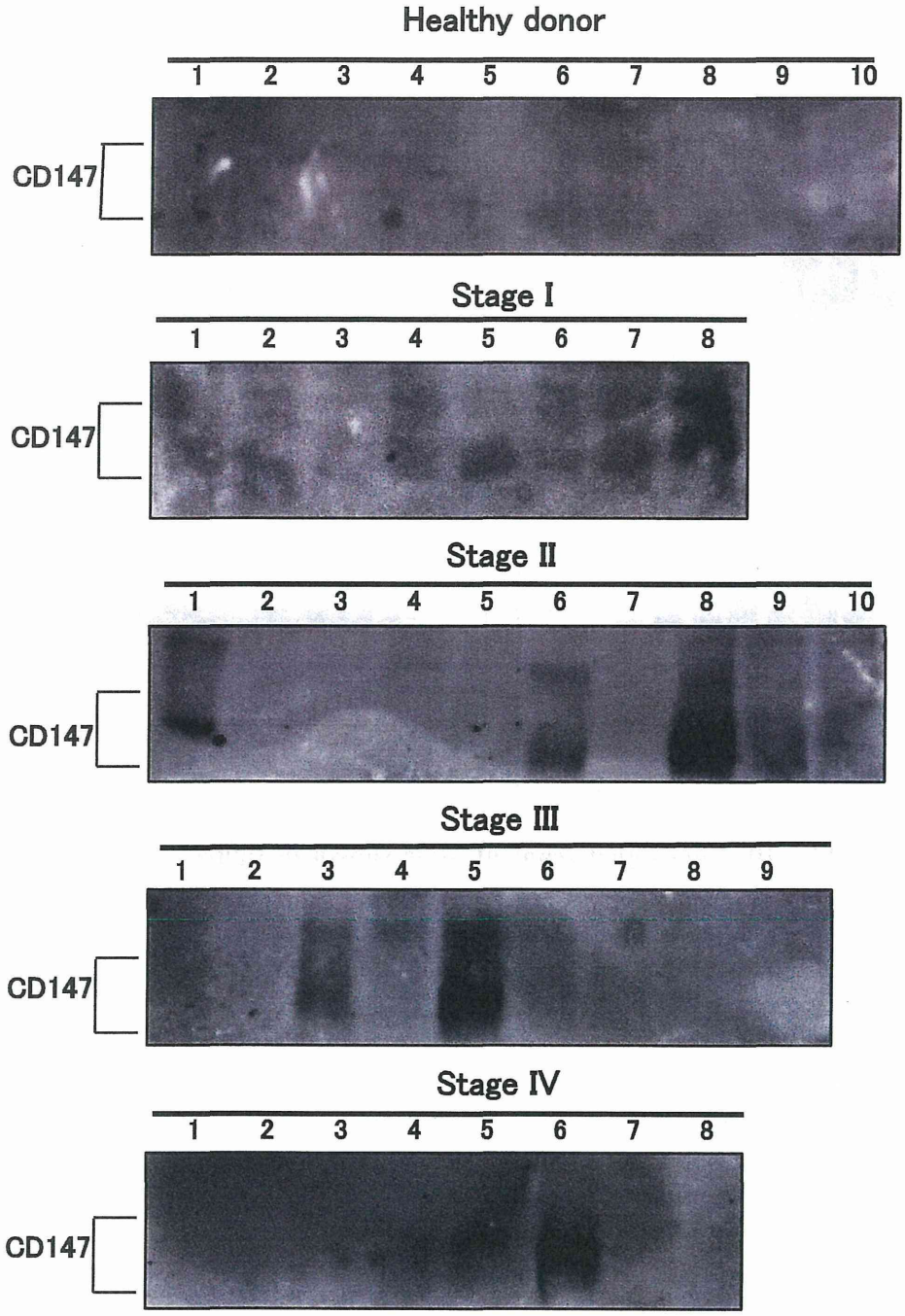

Supplementary Fig. 9. Immunoblotting analysis for CD147 with EVs isolated from colorectal cancer patient serum and healthy control serum. Purified EVs from serum samples that are identical to those in Fig. 6c were employed. Data are representative of at least three independent experiments each.

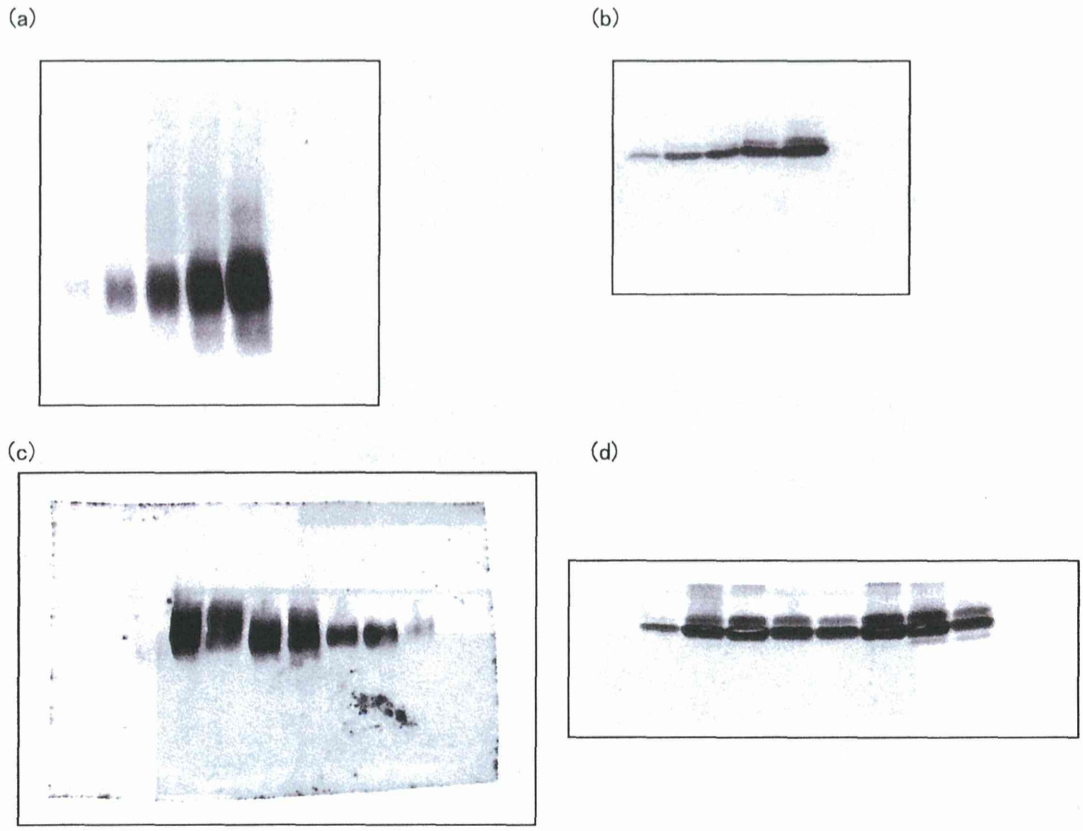

Supplementary Fig. 10. Uncropped scans of blots shown in figures 3a and 5a. (a) Fig.3a, CD63, (b) Fig.3a, CD9, (c) Fig. 5a, CD147, (d) Fig.5a, CD9.

Supplementary Table 1. Membrane proteins selected by proteomic analysis of extracellular vesicles from HCT116 cells and CCD-18Co cells

HCT116 cells

1	Annexin A5
2	Prostaglandin F2 receptor negative regulator
3	Integrin beta-4
4	Moesin
5	Neutral amino acid transporter B(0)
6	Heat shock cognate 71 kDa protein
7	Sodium/potassium-transporting ATPase subunit alpha-1
8	Epithelial cell adhesion molecule
9	CD9 antigen
10	4F2 cell-surface antigen heavy chain
11	Sodium-coupled neutral amino acid transporter 2
12	Integrin beta-1
13	Lactadherin
14	CUB domain-containing protein 1
15	Integrin alpha-3
16	Heat shock protein HSP 90-beta
17	Podocalyxin
18	Monocarboxylate transporter 4
19	Ephrin type-A receptor 2
20	CD63 antigen
21	CD44 antigen
22	CD81 antigen
23	CD151 antigen
24	Basigin (CD147)
25	Tetraspanin-6
26	Tetraspanin-14
27	Choline transporter-like protein 1
28	Solute carrier family 2, facilitated glucose transporter member 1
29	Disintegrin and metalloproteinase domain-containing protein 10
30	Equilibrative nucleoside transporter 1
31	Transferrin receptor protein 1
32	Lysosome-associated membrane glycoprotein 2
33	Heat shock protein beta-1
34	Myoferlin
35	Erythrocyte band 7 integral membrane protein
36	Leucine-rich repeat-containing protein 8B
37	Prominin-1
38	Synaptic vesicle membrane protein VAT-1 homolog
39	Plexin-B2
40	Junctional adhesion molecule A
41	Synaptotagmin-1
42	Protein crumbs homolog 1
43	Integrin alpha-2
44	p53 apoptosis effector related to PMP-22

CCD-18Co cells

1	Lactadherin
2	Annexin A5
3	Erythrocyte band 7 integral membrane protein
4	CD44 antigen
5	Transmembrane protein 176B
6	CD81 antigen
7	CD9 antigen
8	CD63 antigen
9	Thy-1 membrane glycoprotein
10	HLA class I histocompatibility antigen, A-33 alpha chain
11	Heat shock cognate 71 kDa protein
12	Vesicle-associated membrane protein 3
13	Mas-related G-protein coupled receptor member F
14	Transmembrane protein 176A
15	Integrin alpha-1
16	4F2 cell-surface antigen heavy chain
17	CD59 glycoprotein
18	Protein eva-1 homolog B
19	Neutral amino acid transporter B(0)
20	Phospholipid scramblase 3
21	Galectin-1
22	Lipid phosphate phosphohydrolase 3
23	Protein Wnt-7a
24	Amyloid beta A4 protein
25	Uncharacterized protein C17orf80

CD147 is highlighted in yellow and CD9, CD63 and CD81 which are frequently used as EV marker are highlighted in aqua.

After proteomic analysis of EVs from HCT116 cells and CCD-18Co cells, membrane proteins were selected by the descriptions of Gene Ontology which are "integral to plasma membrane", "integral to membrane", "external side of plasma membrane" and "cell surface".
The proteins are listed in the order of protein amount in EVs.

Supplementary Table 2. CEA and CA19-9 in preoperative patient serum (stage 0 and I)

Patient #	signal intensity of CD147/CD9	CEA (ng ml^{-1})	CA19-9 (U ml^{-1})
1	5467	1	6
2	5798	5	6
3	6487	3	5
4	7799	1	13
5	7854	2	13
6	8854	4	26
7	10935	1	25
8	11430	2	21
9	13604	3	6
10	17502	2	18
11	18502	1	13
12	19672	1	11
13	30618	2	5
14	32269	1	5
15	33081	3	9
16	35710	1	26
17	119708	3	12

CEA: Carcinoembrionic Antigen, normal value range is 0–5 ng ml^{-1}.
CA19-9: Carbohydrate Antigen 19-9, normal value range is lower than 37 U ml^{-1}.
An average of the signal intensity of CD147/CD9 in healthy donor serum is 1847.
An average of the signal intensity of CD147/CD9 in cancer patient serum is 6038.
Patients #3, #12 and #17 are stage 0. The other are stage I.

Supplementary Table 3. CEA and CA19-9 in healthy donor serum

Donor #	signal intensity of CD147/CD9	CEA (ng ml^{-1})	CA19-9 (U ml^{-1})
1	484	2	10
2	495	<0.5	8
3	496	2	9
4	525	<0.5	17
5	547	3	<1.0
6	549	3	10
7	557	2	<1.0
8	570	3	25
9	573	<0.5	<1.0
10	583	<0.5	6
11	595	5	18
12	607	4	12
13	620	5	24
14	623	2	9
15	635	2	14
16	652	12	41
17	656	2	40
18	692	<0.5	<1.0
19	692	3	7
20	721	8	<1.0
21	742	148	<1.0
22	749	2	8
23	757	<0.5	4
24	765	2	<1.0
25	773	<0.5	<1.0
26	773	<0.5	48
27	774	3	9
28	774	<0.5	<1.0
29	778	2	14
30	785	3	40
31	785	2	<1.0
32	793	5	9
33	807	5	15
34	809	3	13
35	811	<0.5	9
36	814	3	<1.0
37	828	<0.5	<1.0
38	829	8	12
39	833	5	17
40	833	4	28
41	836	2	6
42	851	3	24
43	872	2	<1.0
44	881	3	15
45	887	7	33
46	890	5	20
47	891	3	10
48	913	<0.5	<1.0
49	932	7	29
50	933	<0.5	5
51	936	3	23
52	943	5	28
53	953	2	<1.0
54	967	<0.5	10
55	970	5	53
56	971	<0.5	8
57	974	5	60
58	986	2	8
59	994	4	9
60	998	<0.5	7
61	999	<0.5	9
62	1005	3	6
63	1008	5	68
64	1016	2	54
65	1019	<0.5	<1.0
66	1020	<0.5	7
67	1021	<0.5	4
68	1022	3	12
69	1023	<0.5	12
70	1028	2	13
71	1031	14	25
72	1036	3	<1.0
73	1039	2	6
74	1053	5	9
75	1055	2	17
76	1057	3	12
77	1058	8	21
78	1073	<0.5	8
79	1074	<0.5	22
80	1076	5	55
81	1084	3	69
82	1085	5	6
83	1092	5	11
84	1096	8	<1.0
85	1097	2	211
86	1116	7	<1.0
87	1118	2	4
88	1129	4	5
89	1155	<0.5	11
90	1178	2	<1.0
91	1190	<0.5	5
92	1199	3	5
93	1212	8	12
94	1213	<0.5	5
95	1230	<0.5	10
96	1231	<0.5	6
97	1235	<0.5	6
98	1239	<0.5	52
99	1252	5	21
100	1263	3	<1.0
101	1275	3	49
102	1295	2	35
103	1296	<0.5	16
104	1306	3	26
105	1311	<0.5	7
106	1316	2	20
107	1352	<0.5	12
108	1358	<0.5	7
109	1364	<0.5	5
110	1366	3	<1.0
111	1371	4	7
112	1397	3	10
113	1398	2	20
114	1411	<0.5	5
115	1427	<0.5	10
116	1435	<0.5	11
117	1437	2	15
118	1451	2	13
119	1455	<0.5	5
120	1457	2	63
121	1459	<0.5	<1.0
122	1462	4	39
123	1493	2	81
124	1512	<0.5	9
125	1512	17	13
126	1513	<0.5	7
127	1522	<0.5	12
128	1530	2	12
129	1533	3	11
130	1538	<0.5	12
131	1556	6	21
132	1563	4	25
133	1569	<0.5	5
134	1583	5	23
135	1583	<0.5	4
136	1586	2	5
137	1593	4	17
138	1612	2	<1.0
139	1614	2	11
140	1628	3	57
141	1643	11	5
142	1653	2	7
143	1713	2	9
144	1718	3	11
145	1720	2	13
146	1746	3	8
147	1749	<0.5	8
148	1754	<0.5	5
149	1758	2	7
150	1766	<0.5	4
151	1774	3	14
152	1776	2	8
153	1816	3	<1.0
154	1816	5	32
155	1828	2	8
156	1839	3	<1.0
157	1846	4	9
158	1860	<0.5	9
159	1867	2	<1.0
160	1878	3	3
161	1897	2	9
162	1968	<0.5	6
163	2002	3	<1.0
164	2003	3	22
165	2036	<0.5	13
166	2063	<0.5	6
167	2073	3	15
168	2075	2	24
169	2147	2	23
170	2193	4	16
171	2215	2	16
172	2380	<0.5	27
173	2383	3	21
174	2399	<0.5	33
175	2512	3	23
176	2525	<0.5	5
177	2563	<0.5	5
178	2685	2	28
179	2783	6	3
180	2870	<0.5	15
181	2986	<0.5	5
182	3005	<0.5	29
183	3124	2	16
184	3367	<0.5	7
185	4145	3	5
186	4243	<0.5	6
187	4309	<0.5	4
188	4322	<0.5	6
189	4906	2	20
190	11760	2	10
191	76476	2	<1.0

CEA: Carcinoembrionic Antigen, normal value range is 0–5 ng ml^{-1}.
CA19-9: Carbohydrate Antigen 19-9, normal value range is lower than 37 U ml^{-1}.
Exceeding the normal value range are presented in red text.

STEM CELLS

CANCER STEM CELLS

Clinical Relevance and Therapeutic Significance of MicroRNA-133a Expression Profiles and Functions in Malignant Osteosarcoma-Initiating Cells

TOMOHIRO FUJIWARA,[a,b,c] TAKESHI KATSUDA,[a] KEITARO HAGIWARA,[a] NOBUYOSHI KOSAKA,[a] YUSUKE YOSHIOKA,[a] RYOU-U TAKAHASHI,[a] FUMITAKA TAKESHITA,[a] DAISUKE KUBOTA,[d] TADASHI KONDO,[d] HITOSHI ICHIKAWA,[e] AKIHIKO YOSHIDA,[f] EISUKE KOBAYASHI,[b] AKIRA KAWAI,[b] TOSHIFUMI OZAKI,[c] TAKAHIRO OCHIYA[a]

Key Words. Osteosarcoma • MicroRNA • Locked nucleic acid • Clinical translation

ABSTRACT

Novel strategies against treatment-resistant tumor cells remain a challenging but promising therapeutic approach. Despite accumulated evidence suggesting the presence of highly malignant cell populations within tumors, the unsolved issues such as *in vivo* targeting and clinical relevance remain. Here, we report a preclinical trial based on the identified molecular mechanisms underlying osteosarcoma-initiating cells and their clinical relevance. We identified key microRNAs (miRNAs) that were deregulated in a highly malignant CD133^{high} population and found that miR-133a regulated the cell invasion that characterizes a lethal tumor phenotype. Silencing of miR-133a with locked nucleic acid (LNA) reduced cell invasion of this cell population, and systemic administration of LNA along with chemotherapy suppressed lung metastasis and prolonged the survival of osteosarcoma-bearing mice. Furthermore, in a clinical study, high expression levels of CD133 and miR-133a were significantly correlated with poor prognosis, whereas high expression levels of the four miR-133a target genes were correlated with good prognosis. Overall, silencing of miR-133a with concurrent chemotherapy would represent a novel strategy that targets multiple regulatory pathways associated with metastasis of the malignant cell population within osteosarcoma. STEM CELLS *2014;32:959–973*

[a]Division of Molecular and Cellular Medicine, National Cancer Center Research Institute, Tokyo, Japan; [b]Department of Musculoskeletal Oncology, National Cancer Center Hospital, Tokyo, Japan; [c]Department of Orthopedic Surgery, Okayama University Graduate School of Medicine, Dentistry, and Pharmaceutical Sciences, Okayama, Japan; [d]Division of Pharmacoproteomics, National Cancer Center Research Institute, Tokyo, Japan; [e]Division of Genetics, National Cancer Center Research Institute, Tokyo, Japan; [f]Division of Pathology and Clinical Laboratories, National Cancer Center Hospital, Tokyo, Japan

Correspondence: Takahiro Ochiya, Ph.D., Division of Molecular and Cellular Medicine, National Cancer Center Research Institute, 5-1-1, Tsukiji, Chuo-ku, Tokyo 104-0045, Japan. Telephone: +81-3-3542-2511, ext. 4800; Fax: +81-3-5565-0727; e-mail: tochiya@ncc.go.jp

Received July 8, 2013; accepted for publication November 22, 2013; first published online in STEM CELLS *EXPRESS* December 19, 2013.

1066-5099/2014/$30.00/0

http://dx.doi.org/10.1002/stem.1618

INTRODUCTION

Sarcomas are distinctly heterogeneous tumors [1, 2]. Although the origin of sarcomas remains unknown, the overwhelming number of histopathological types and subtypes implies that sarcomas are a "stem cell malignancy" with multilineage differentiation abilities that result from dysregulated self-renewal [3]. The cancer stem cell theory, which states that a subset of cells within a tumor have stem-like phenotypes such as self-renewal and differentiation, has introduced a novel biological paradigm for many human tumors [4, 5]. These cancer stem cells (CSCs) or tumor-initiating cells (TICs) have been proposed to cause tumor recurrence and metastasis because of their lethal characteristics, including drug resistance, invasion, and tumorigenicity [6, 7]. Therefore, the development of TIC-targeted therapy would provide new hope for cancer patients, but these treatments have not reached the clinic.

Osteosarcoma is the most common primary bone malignancy [2, 8]. Along with the development of multiagent chemotherapy and surgical techniques including the concepts of surgical margins [9] and reconstruction [10], patient prognosis has gradually improved over the past 30 years. However, for patients who present with metastatic disease, the outcomes are far worse, with survival rates below 30%, within 5 years of diagnosis [11]. Furthermore, some cases present with distant metastases long after the initial treatment [12]. Considering these clinical characteristics and histopathological heterogeneity, emerging reports have implicated a role for osteosarcoma TICs [13–21]. However, the molecular mechanisms underlying the phenotypes of TICs and the importance of this population in clinical situations have not been elucidated. In this study, we focused on the multiple pathways within TICs in view of microRNA (miRNA) regulation.

Emerging evidence suggests that cancer initiation and progression involve miRNAs, which are small noncoding single-stranded RNAs of 20–22 nucleotides that negatively regulate gene expression at the post-transcriptional level through imperfect base paring with the 3′ untranslated region (UTR) of their target mRNA [22]. These miRNAs are

central to RNA interference (RNAi) [23]. The biogenesis of miRNAs involves a complex protein system, including members of the Argonaute family, Pol II-dependent transcription, and the RNase IIIs Drosha and Dicer [24]. Growing evidence suggests that miRNAs are involved in crucial biological processes, including development, differentiation, apoptosis, and proliferation [24]. Numerous profiling studies of miRNAs have revealed that deregulation of miRNA may contribute to many types of human diseases, including cancer. Depending on the target mRNAs that they regulate, miRNAs can function as tumor promoters or suppressors, regulating the maintenance and progression of cancers and TICs [25, 26]. In addition, miRNA expression profiles have been correlated with the tumor stage, progression, and prognosis of cancer patients [27, 28]. These findings indicate that miRNAs are critical regulators of tumor development and progression.

To date, the molecular mechanisms underlying the tumor-initiating phenotypes of osteosarcoma, their clinical correlations, and effective treatments against them have not been elucidated. In this study, we confirmed that the osteosarcoma $CD133^{high}$ cell population not only demonstrate a tumor-initiating phenotype but also show significant correlation with poor prognoses for osteosarcoma patients. In addition, we elucidated that miR-133a is a key regulator of cell invasion, which constitutes these malignant phenotypes of osteosarcoma, and that silencing of miR-133a with locked nucleic acid (LNA) inhibited osteosarcoma metastasis *in vivo* when applied with current chemotherapy. Furthermore, the expression of miR-133a and its target genes significantly correlated with the prognoses of osteosarcoma patients. Thus, our preclinical trial using LNA therapeutics may represent a novel strategy for osteosarcoma treatment through regulating multiple molecular pathways of the malignant cell population within osteosarcoma.

Materials and Methods

Osteosarcoma Cell Purification from Fresh Clinical Samples

Fresh human osteosarcoma samples were obtained in accordance with the ethical standards of the Institutional Committee on Human Experimentation from two patients who were undergoing diagnostic incisional biopsy from primary sites of osteosarcoma prior to receiving neoadjuvant chemotherapy at the National Cancer Center Hospital of Japan between October 2010 and June 2011. The osteosarcoma diagnosis and the histological subtypes were determined by certified pathologists. The surgical specimens were obtained at the time of resection and were received in the laboratory within 10 minutes, immediately mechanically disaggregated, digested with collagenase (Nitta Gelatin, Osaka, Japan, http://www.nitta-gelatin.co.jp) and washed twice with phosphate-buffered saline (PBS). The cells were cultured in Dulbecco's modified Eagle's medium (DMEM) (Life Technologies, Carlsbad, CA, http://www.lifetech.com) containing 10% heat-inactivated fetal bovine serum (FBS) (Life Technologies), penicillin (100 U/mL), and streptomycin (100 μg/mL) in 5% CO_2 in a humidified incubator at 37°C.

Cells and Cell Culture

The human osteosarcoma cell lines SaOS2, U2OS, MG63, HOS, MNNG/HOS, and 143B were purchased from the American Type Culture Collection (ATCC, Manassas, VA, http://www.atcc.org). The human osteosarcoma cell lines HuO9 and 143B-luc were previously established in our laboratory [29, 30], and SaOS2-luc cell line, a stable luciferase-expressing cell line, was newly established using a plasmid vector. We cultured SaOS2, SaOS-luc, and HuO9 cells in RPMI 1640 (Life Technologies). U2OS, MG63, HOS, MNNG/HOS, 143B, and 143B-luc cells were cultured in DMEM. All media were supplemented with 10% heat-inactivated FBS (Life Technologies), penicillin (100 U/mL), and streptomycin (100 μg/mL). The cells were maintained under 5% CO_2 in a humidified incubator at 37°C.

Cell Sorting and Flow Cytometry

Cell sorting by flow cytometry was performed on osteosarcoma cell lines and clinical samples using allophycocyanin (APC)-conjugated monoclonal mouse anti-human CD133/2 (293C3, Miltenyi Biotec, Auburn, CA, https://www.miltenyibiotec.com) and phycoerythrin (PE)-conjugated monoclonal mouse anti-human CD44 (eBioscience, San Diego, CA, http://www.ebioscience.com) antibodies. Isotype control mouse IgG2b-APC (Miltenyi Biotec) and mouse IgG2b-PE (eBioscience) served as a control. The samples were analyzed and sorted on a JSAN cell sorter (Bay Bioscience, Kobe, Japan, http://www.baybio.co.jp) and a BD FACS Aria II (BD Biosciences, Tokyo, Japan, http://www.bdbiosciences.com). Viability was assessed using propidium iodide (PI) to exclude dead cells. The results were analyzed using FlowJo software (Tree Star, San Carlos, CA, http://www.treestar.com).

Cell Proliferation and Cytotoxicity Assays

The cell proliferation rates and cell viability were used as indicators of the relative sensitivity of the cells to doxorubicin (DOX), cisplatin (CDDP), and methotrexate (MTX), and these measurements were determined using the TetraColor ONE Cell Proliferation Assay (Seikagaku, Tokyo, Japan, http://www.seikagaku.co.jp/) or Cell proliferation kit 8 (Dojindo, Kumamoto, Japan, http://www.dojindo.co.jp), according to the manufacturer's instructions. Cells growing in the logarithmic phase were seeded in 96-well plates (3×10^3 per well), allowed to attach overnight, and then treated with varying doses of doxorubicin (Sigma-Aldrich, St. Louis, MO, http://www.sigmaaldrich.com), CDDP (Enzo Life Sciences, Farmingdale, NY, http://www.enzolifesciences.com), or MTX (Sigma-Aldrich) for 72 hours in triplicate. The absorbance was measured at 450 nm with a reference wavelength at 620 nm using EnVision (Perkin-Elmer, Waltham, MA, http://www.perkinelmer.com). The relative number of viable cells was expressed as the percent of viable cells.

Sphere Formation

Freshly isolated $CD133^{high}$ and $CD133^{low}$ osteosarcoma SaOS2 cells were plated on ultra low-attachment 96-well plates (Corning, Corning, NY, http://www.corning.com) at a concentration of a single cell per well containing 100 μL of culture medium, which was confirmed visually. Wells containing either no cells or more than one cell were excluded for further analysis. The ratios of the wells containing spheres formed from single cells on day 10 were counted. The wells containing the cells that did not form spheres were excluded. The numbers of spheroids were counted 10 days after cell sorting. Serum-free DMEM/F12 (Life Technologies) supplemented with

20 ng/mL human recombinant epidermal growth factor (Sigma-Aldrich), 10 ng/mL human recombinant basic fibroblast growth factor (Life Technologies), 4 μg/mL insulin (Sigma-Aldrich), B27 (1:50; Life Technologies), 500 units/mL penicillin (Life Technologies) and 500 μg/mL streptomycin (Life Technologies) was used as the culture medium.

Invasion Assay

Invasion assays were performed using 24-well BD BioCoat Invasion Chambers with Matrigel (BD). A total of 1×10^5 cells were suspended in 500 μL DMEM or RPMI 1640 medium without FBS and added to the upper chamber. DMEM or RPMI 1640 medium with 10% FBS was added to the lower chamber. After incubation for 24 or 36 hours, the cells on the upper surface of the filter were completely removed by wiping with cotton swabs. The filters were fixed in methanol and stained with 1% toluidine blue in 1% sodium tetraborate (Sysmex, Kobe, Japan, http://www.sysmex.co.jp). The filters were mounted onto slides, and the cells on the lower surfaces were counted.

miRNA Profiling

miRNA expression profiling was performed using a miRNA microarray manufactured by Agilent Technologies (Santa Clara, CA, http://www.home.agilent.com) that contained 866 human miRNAs. Three independently extracted RNA samples obtained from $CD133^{high}$ and $CD133^{low}$ cells just after isolation were used for the array analyses. The labeling and hybridization of the total RNA samples were performed according to the manufacturer's protocol. The microarray results were extracted using the Agilent Feature Extraction software (v10.7.3.1) and analyzed using GeneSpring GX 11.0.2 software (Agilent Technologies).

Clinical Samples for Correlating Survival with the Expression of CD133, MiR-133a, and Targets of MiR-133a

The osteosarcoma tissue samples were obtained from diagnostic incisional biopsies of primary osteosarcoma sites before the start of neoadjuvant chemotherapy at the National Cancer Center Hospital of Japan between June 1997 and September 2010. We did not include patients older than 40 years or patients who had primary tumors located outside the extremities. Each fresh tumor sample was cut into two pieces; one piece was immediately cryopreserved in liquid nitrogen, and the other piece was fixed in formalin. The osteosarcoma diagnosis and the histological subtypes were determined by certified pathologists. Only osteosarcoma samples with the osteoblastic, chondroblastic, fibroblastic, or telangiectatic subtypes were included. The response to chemotherapy was classified as good if the tumor necrosis was 90% or greater. To correlate the survival studies with the expression of CD133 and the targets of miR-133a, 35 available cDNA samples from the cDNA library were used, and RNA from 48 available formalin-fixed paraffin-embedded (FFPE) samples were used for the correlation study with miR-133a expression. The patient clinical information is summarized in Supporting Information Table S1 and S2. All patients provided written, informed consent authorizing the collection and use of their samples for research purposes. The study protocol for obtaining clinical information and collecting samples was approved by the Institutional Review Board of the National Cancer Center of Japan.

RNA Isolation and Quantitative Real-Time Reverse Transcriptase Polymerase Chain Reaction of mRNAs and miRNAs

We purified total RNA from cells and tumor tissues using the miRNeasy Mini Kit (Qiagen, Valencia, CA, http://www.qiagen.com). For quantitative polymerase chain reaction (qPCR) of mRNAs, cDNA was synthesized using a High-Capacity cDNA Reverse Transcription Kit (Life Technologies). For each qPCR, equal amounts of cDNA were mixed with Platinum SYBR Green qPCR SuperMix (Life Technologies) and the specific primers (Supporting Information Table S3). We normalized gene expression levels to β-actin or GAPDH. For the qPCR of miRNAs, miRNA was converted to cDNA using the TaqMan MicroRNA Reverse Transcription Kit (Life Technologies). RNU6B small nuclear RNA was amplified as an internal control. qPCR was performed using each miRNA-specific probe included with the TaqMan MicroRNA Assay. The reactions were performed using a Real-Time PCR System 7300 with the SDS software (Life Technologies).

Transfection with Synthetic miRNAs, LNAs, and siRNAs

Synthetic hsa-miRs (Pre-miR-hsa-miR-1, 10b, 133a, and negative control (NC); Life Technologies; Supporting Information Table S4) and LNAs (LNA-1, 10b, 133a, and negative control; Exiqon, Vedbæk, Denmark, http://www.exiqon.com and Gene Design, Ibaraki, Japan, http://www.genedesign.co.jp, Supporting Information Table S5) were transfected into each cell line at 30 nM each (final concentration) using DharmaFECT one (Thermo Scientific, Yokohama, Japan, http://www.thermoscientific.jp). The synthetic siRNAs (Bonac Corporation, Kurume, Japan, http://www.bonac.com, Supporting Information Table S6) were transfected into cells at 100 nM each (final concentration) using DharmaFECT one (Thermo Scientific). After 24 hours of incubation, the cells were harvested and reseeded into a 6-well or 96-well plate.

Tumor Transplantation Experiments

The animal experiments in this study were performed in compliance with the guidelines of the Institute for Laboratory Animal Research at the National Cancer Center Research Institute. Athymic nude mice or NOD/SCID mice (CLEA Japan, Tokyo, Japan, http://www.clea-japan.com) were purchased at 4 weeks of age and given at least 1 week to adapt to their new environment prior to tumor transplantation. On day 0, the mice were anesthetized with 3% isoflurane, and the right leg was disinfected with 70% ethanol. The cells were aspirated into a 1 mL tuberculin syringe fitted with a 27-G needle. The needle was inserted through the cortex of the anterior tuberosity of the tibia with a rotating movement to avoid cortical fracture. Once the bone was traversed, the needle was inserted further to fracture the posterior cortex of the tibia. A 100 μL volume of solution containing SaOS2-luc cells (10^2, 10^3, 10^4, 10^5) or 143B-luc cells (1.5×10^6) was injected while slowly removing the needle.

Monitoring Tumor Growth, Lung Metastasis, and Toxicity with/Without LNA-Anti-MiR-133a

To evaluate LNA-133a administration to mice with spontaneous osteosarcoma lung metastases, individual mice were

injected with 10 mg/kg of LNA-133a or control LNA-NC (LNA-negative control) via the tail vain. LNAs were injected on days 4, 11, 18 postinoculation with the 143B-luc cells, followed by intraperitoneal injection of 3.5 mg/kg of CDDP on days 5, 12, and 19. Each experimental condition included 10 animals per group. The development of subsequent lung metastases was monitored once per week *in vivo* using bioluminescent imaging for 3 weeks. All data were analyzed using LivingImage software (version 2.50, Xenogen, Alameda, CA). On day 22, the primary tumors and lungs of five mice in each group were resected at necropsy for weight, bioluminescence, and histological analyses. A blood examination, weighing of the whole body, heart, liver, and skeletal muscle, and a histopathological examinations were performed for toxicity assessment. The remaining mice were observed for survival.

Comprehensive Collection and Identification of MiR-133a Target mRNAs

To identify comprehensive downstream targets of miR-133a, we performed cDNA microarray profiling using two experimental approaches. First, we collected candidate genes from the cDNA microarray analysis performed on total RNA collected from SaOS2 $CD133^{low}$ cells transfected with miR-133a or NC. Second, a cDNA microarray analysis was performed on total RNA collected using anti-Ago2 antibody immunoprecipitation (Ago2-IP) from $CD133^{low}$ cells transduced with miR-133a or NC. The genes that were identified in the former method as downregulated with a 1.5-fold decrease and the genes identified in the latter method as upregulated with a 2-fold increase were defined as candidates by reference to *in silico* databases using TargetScanHuman 6.0 (http://www.targetscan.org).

Luciferase Reporter Assays

Each fragment of the 3′ UTR of sphingomyelin synthase 2 (SGMS2) (nt 1,656–1,879 of NM_152621), ubiquitin-like modifier activating enzyme 2 (UBA2) (nt 2,527–2,654 of NM_005499), sorting nexin family member 30 (SNX30) (nt 6,659–7,611 of NM_001012944), and annexin A2 (ANXA2) (nt 1,056–1,634 of NM_001002857) were amplified and cloned into the XhoI and NotI sites of a psiCHECK-2 vector containing either the firefly or Renilla luciferase reporter gene (Promega, Tokyo, Japan, http://www.promega.com). We verified all PCR products that were cloned into the plasmid using DNA sequencing to ensure that they were free of mutations and in the correct cloning direction. The primer sequences are listed in Supporting Information Table S7. For the luciferase reporter assay, SaOS2 cells were cotransfected with 100 ng of luciferase constructs and 100 nM synthetic miR-133a molecules or control (nontargeting siRNA oligonucleotide, Qiagen). The firefly and Renilla luciferase activity levels were measured using the Dual-Luciferase Reporter Assay (Promega) 48 hours after transfection. The results are expressed as relative Renilla luciferase activity (Renilla luciferase/firefly luciferase).

Immunohistochemistry

To stain the miR-133a targets, we prepared slides from osteosarcoma xenograft tumors. Endogenous peroxidase was quenched with 1% H_2O_2 (30 minutes). The slides were heated for antigen retrieval in 10 mM sodium citrate (pH 6.0). Subsequently, we incubated the slides with monoclonal mouse anti-human SGMS2 (1:50 dilution, Abcam, Tokyo, Japan, http://www.abcam.co.jp), ANXA2 (1:250 dilution, Abcam), or isotype-matched control antibodies overnight at 4°C. Immunodetection was performed using ImmPRESS peroxidase polymer detection reagents (Vector Labs, Burlingame, CA, https://www.vectorlabs.com) and the Metal-Enhanced DAB Substrate Kit (Thermo Scientific) in accordance with the manufacturer's directions. The sections were counterstained with hematoxylin for contrast.

Statistical Analyses

All statistical analyses were performed using SPSS Statistics Version 21 software (IBM SPSS, Tokyo, Japan, https://www.ibm.com). Student's t test or one-way ANOVA, corrected for multiple comparisons as appropriate, was used to determine the significance of any differences between experimental groups. The differences in CD133, miR-133a, and the miR-133a targets expression among different clinicopathological data were analyzed using the chi-squared (χ^2) test or ANOVA. We carried out receiver-operating characteristic curve analysis using the SPSS software, and the optimal cutoff points for the expression levels of CD133, miR-133a, and the target genes of miR-133a were determined by the Youden index, that is, $J = \max$ (sensitivity + specificity − one) [31]. The Kaplan-Meier method and the log-rank test were used to compare the survival of patients. We defined the survival period as the time from diagnosis until death, whereas living patients were censored at the time of their last follow-up. For all the analyses, we considered a p value of .05 or less to be significant.

Results

Osteosarcoma $CD133^{high}$ Cell Populations Are Enriched with Highly Malignant Cells with the Multiple Phenotypes

Based on the emerging evidence that tumors contain the heterogeneous cell populations, we tried to isolate the small population of highly malignant cells in osteosarcoma. In order to evaluate the phenotypes of the cell population, we screened human osteosarcoma cell lines (SaOS2, U2OS, HOS, MG-63, HuO9, MNNG/HOS, and 143B) for the markers expressed on the highly malignant cell populations within the tumors [4, 7, 32]. As a result, we confirmed that CD133, a human structural homolog of mouse prominin-1, was expressed in a small proportion of cells ranging from 0.04% to 8.47% (Fig. 1A; Supporting Information Fig. S1A), which was consistent with the previous reports [18, 19]. Several examinations were performed to confirm the phenotypes of the SaOS2 $CD133^{high}$ and $CD133^{low}$ populations. Freshly isolated $CD133^{high}$ and $CD133^{low}$ osteosarcoma SaOS2 cells were plated at a concentration of a single cell and cultured immediately in a serum-free, growth factor-supplemented, anchorage-independent environment. Within 2 weeks of culture, we observed more osteosarcoma spheres from the $CD133^{high}$ cells than from the $CD133^{low}$ cells (Fig. 1B, 1C). The cell proliferation rate was slightly lower in $CD133^{high}$ cell population than in $CD133^{low}$ cell population (Supporting Information Fig. S1D). To assess the difference of drug resistance, both populations were observed after exposure to doxorubicin (DOX), cisplatin (CDDP), or methotrexate (MTX), which are the standard

